
Article

An Assessment of Global Dimming and Brightening during 1984–2018 Using the FORTH Radiative Transfer Model and ISCCP Satellite and MERRA-2 Reanalysis Data

Michael Stamatis ¹, Nikolaos Hatzianastassiou ^{1,*}, Marios-Bruno Korras-Carraca ^{1,2}, Christos Matsoukas ³, Martin Wild ⁴ and Ilias Vardavas ⁵

¹ Laboratory of Meteorology & Climatology, Department of Physics, University of Ioannina, 45110 Ioannina, Greece; m.stamatis@uoi.gr (M.S.); koras@env.aegean.gr (M.-B.K.-C.)

² Institute for Astronomy, Astrophysics, Space Applications and Remote Sensing, National Observatory of Athens, 11810 Athens, Greece

³ Department of Environment, University of the Aegean, 81100 Mytilene, Greece; matsoukas@aegean.gr

⁴ Institute for Atmospheric and Climate Science, ETH Zürich, 8092 Zürich, Switzerland; martin.wild@env.ethz.ch

⁵ Department of Physics, University of Crete, 71003 Heraklion, Greece; vardavas@uoc.gr

* Correspondence: nhatzian@uoi.gr

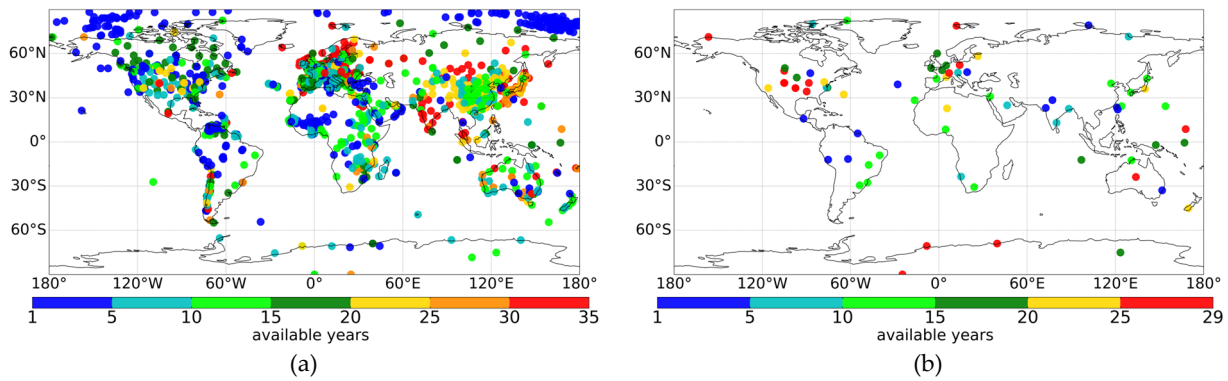


Figure S1. Global distribution of: (a) Global Energy Balance Archive (GEBA) 1545 stations and (b) Baseline Surface Radiation Network (BSRN) 73 stations, initially accessible for the evaluation of the FORTH-RTM surface solar radiation (SSR) data. The availability of each station's monthly data in years is indicated in the colorbars.

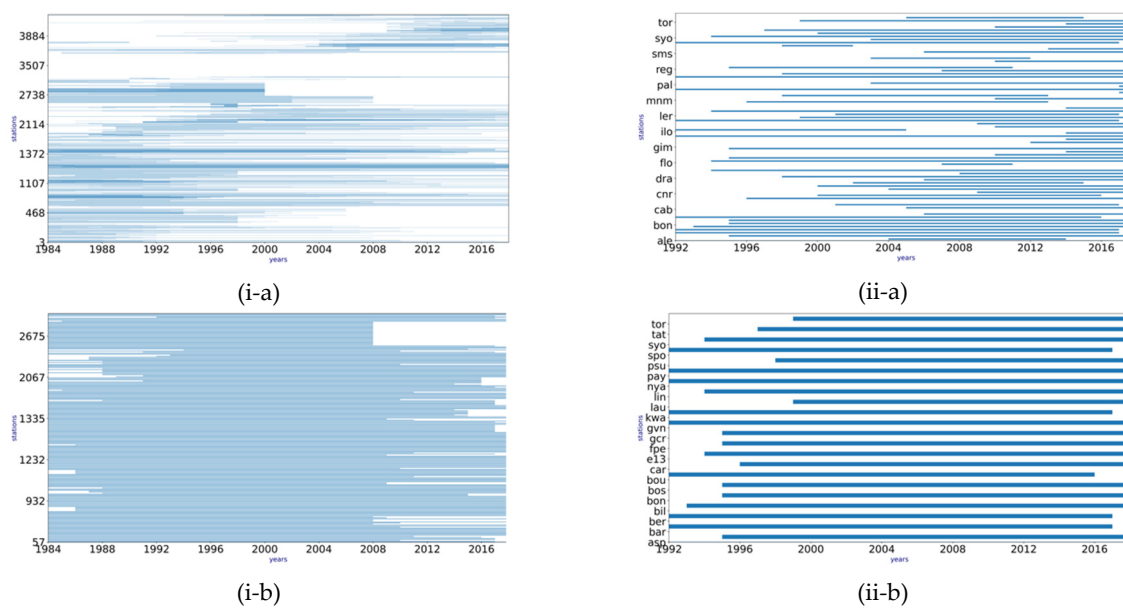


Figure S2. Time periods covered by measurements of each station of (i) GEBA (1545 stations) and (ii) BSRN (73 stations) networks. Results are given for (a) the total number of stations since 1984 and (b) the number of available stations after applying criteria for computing linear slopes (see Section 2.2 of main paper), i.e., 222 GEBA and 22 BSRN stations.

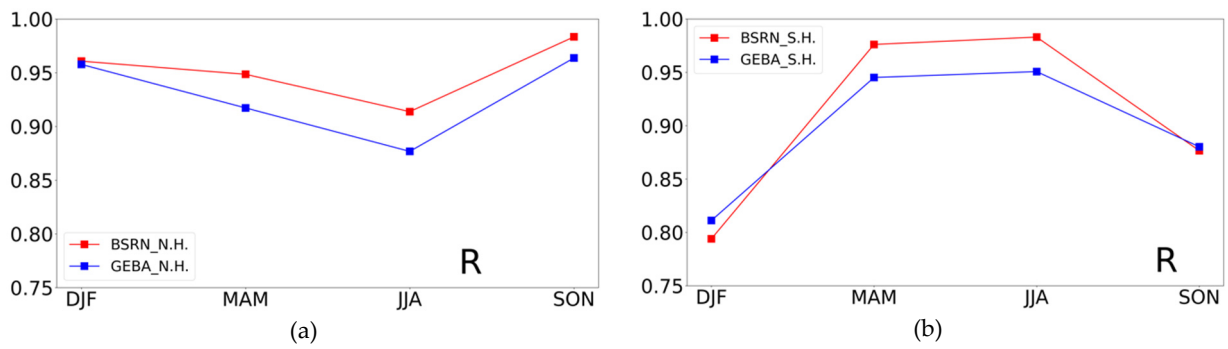


Figure S3. Seasonal variation of hemispherical mean correlation coefficient R between FORTH-RTM and GEBA (blue color) and between FORTH-RTM and BSRN (red color) stations, computed using SSR fluxes for the North Hemisphere (a) and the South Hemisphere (b).

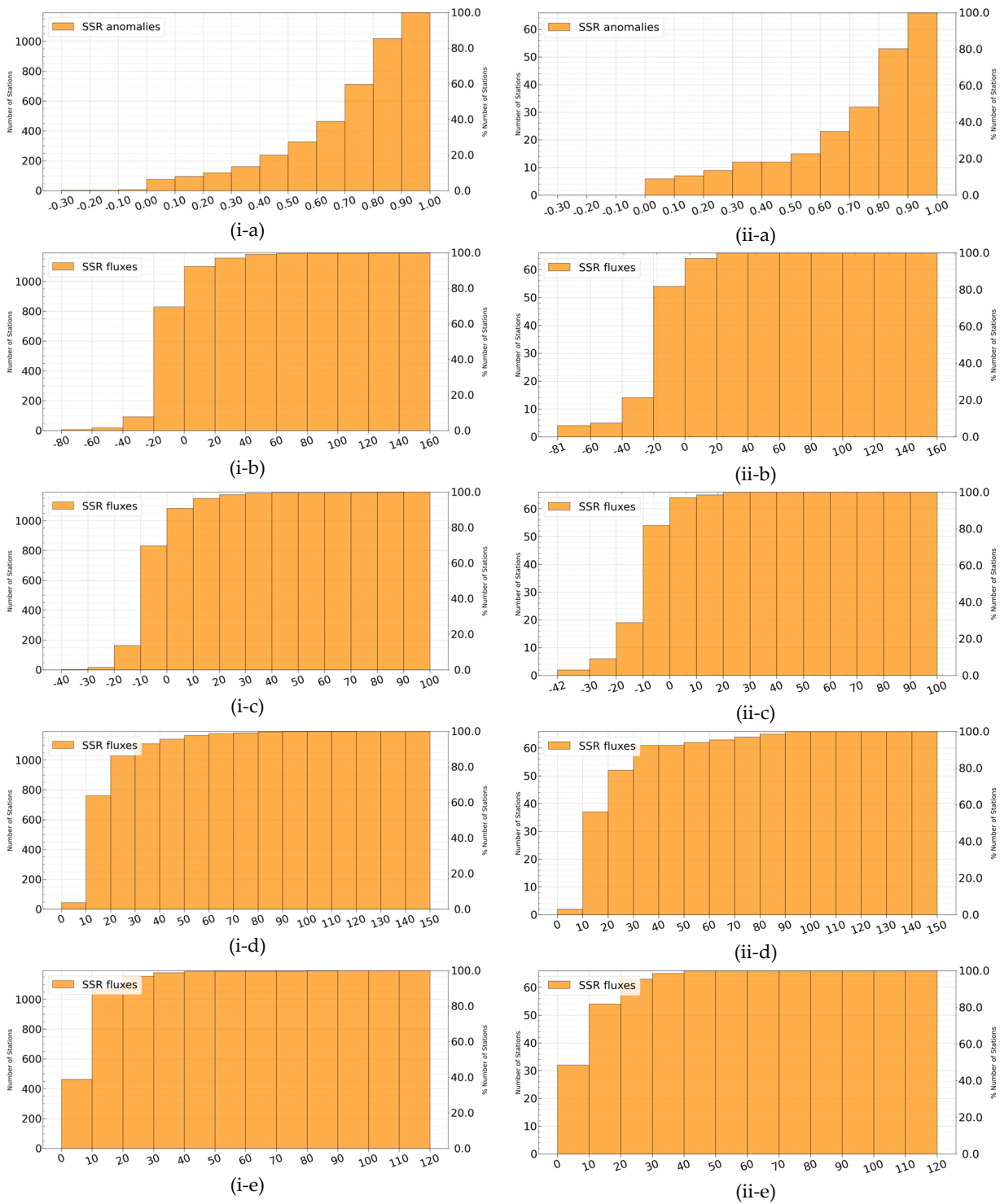


Figure S4. Cumulative histogram distribution of correlation coefficient R (a), bias (b), relative bias (c), root mean squared error (RMSE) (d), relative RMSE (e), between FORTH and GEBA (i, left column) and BSRN (ii, right column) stations. Results are computed using FORTH-RTM, and GEBA and BSRN station SSR fluxes, except for R , which is computed using deseasonalized SSR anomalies. In the left y axis shown is the number of stations, while in the right y axis the % number of stations.

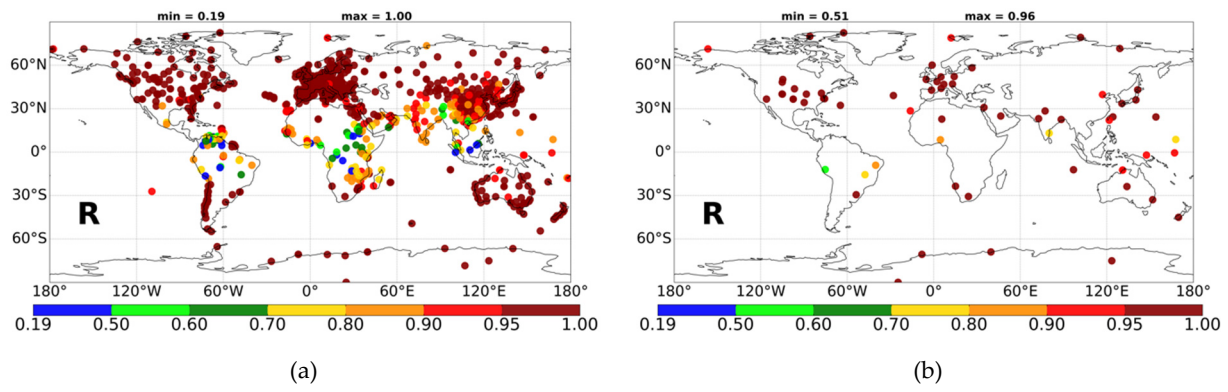


Figure S5. Global distribution of correlation coefficient between FORTH-RTM and each GEBA (a, left column) and BSRN (b, right column) station SSR fluxes.

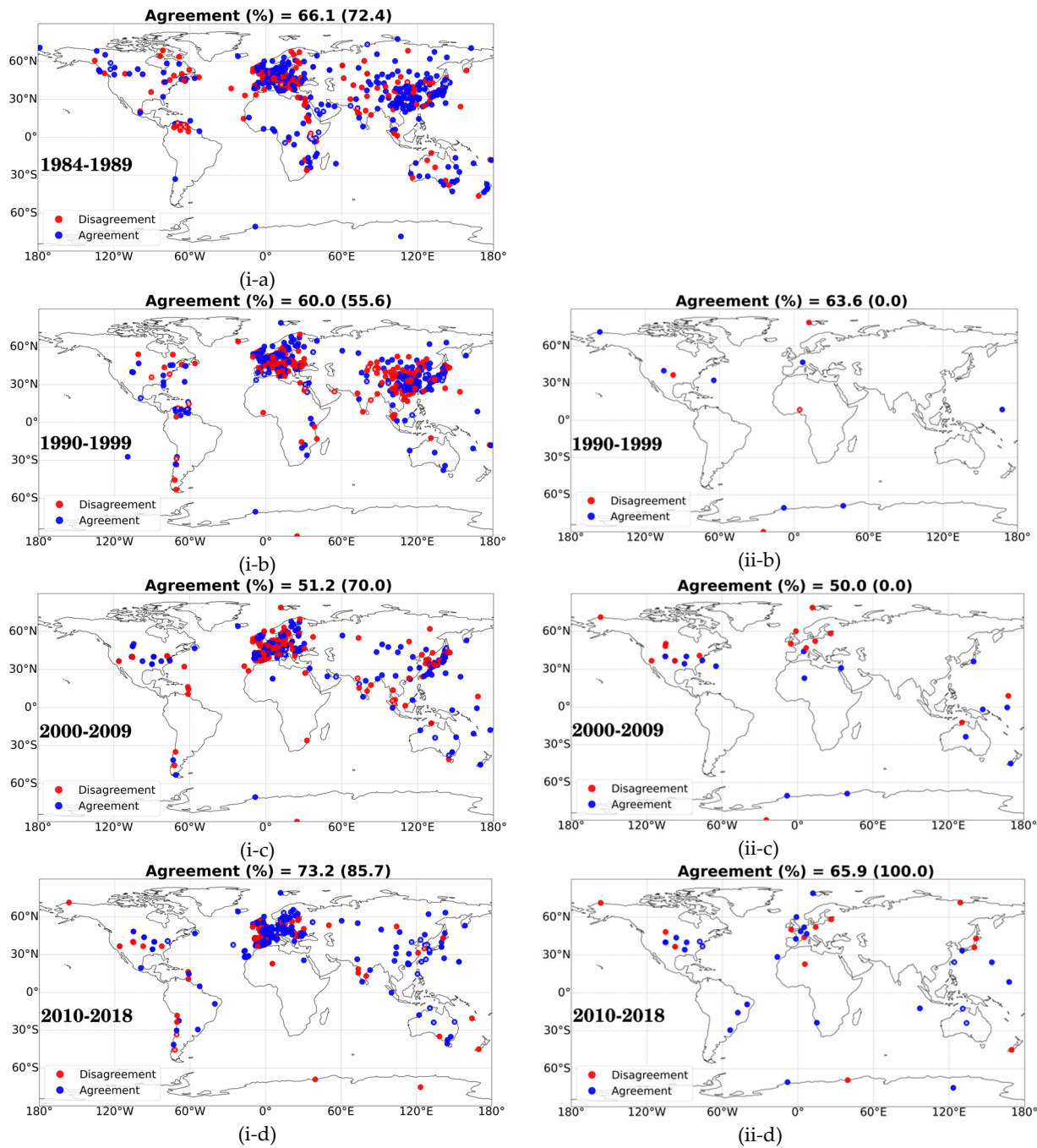


Figure S6. Agreement (blue dots) and disagreement (red dots) between FORTH-RTM and station GDB ($\Delta(SSR)$). The comparison is done using deseasonalized anomalies for model and GEBA (left column, i) and BSRN (right column, ii) station fluxes per selected time periods that are characterized as Global Dimming & Brightening periods (GDB phases). The embedded white x symbols indicate the statistically significant trends. At the top of each figure is indicated the percent number of stations for which there is agreement in GDB, with respect to the overall number of stations. The numbers in parentheses provide the agreement of statistically significant trends. The GDB phases (according to Wild et al., WIREs Clim. Change 2016, 7:91-107) are: (a) 1984–1989, (b) 1990–1999, (c) 2000–2009, (d) 2010–2018 for GEBA and (a) 1992–1999, (b) 2000–2009, (c) 2010–2018 for BSRN.

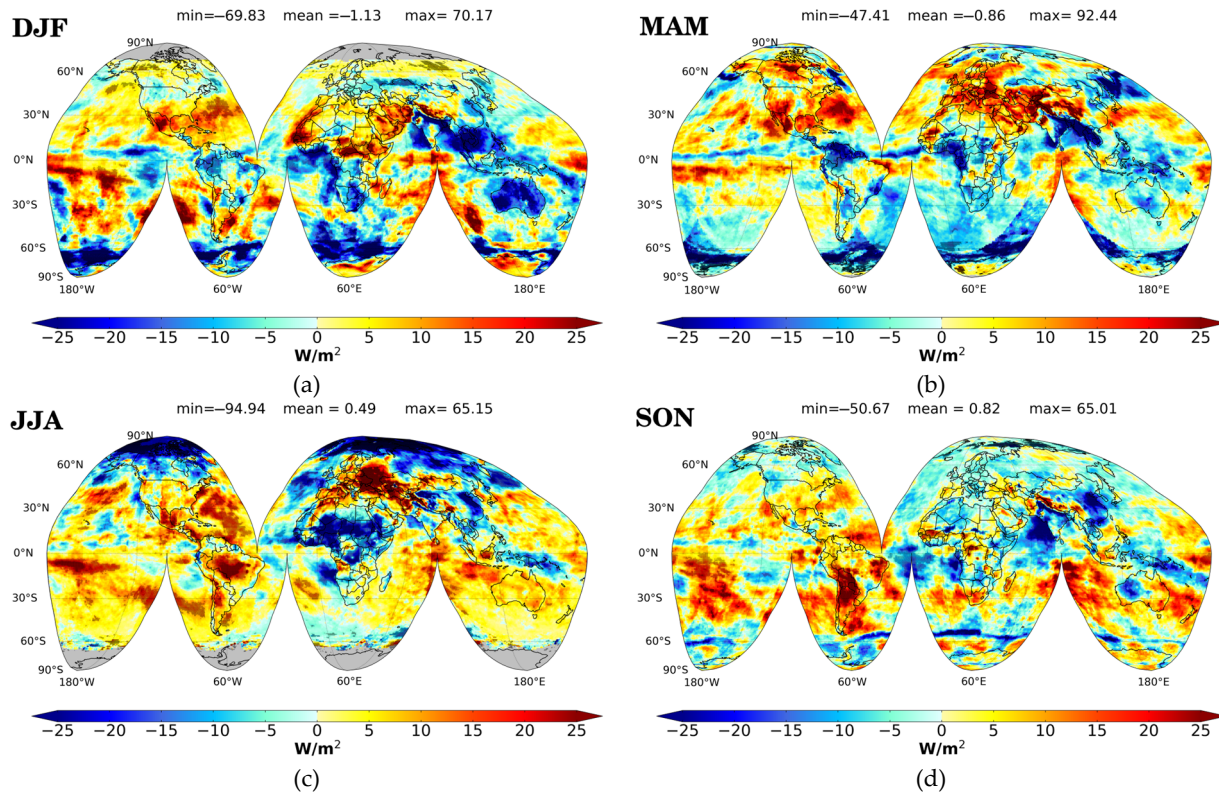


Figure S7. Global distribution of FORTH-RTM GDB [$\Delta(\text{SSR})$] over the 35-year period 01/1984 – 12/2018, for (a) DJF, (b) MAM, (c) JJA, (d) SON. Reddish colors are those with positive trends (brightening), and those with bluish colors have negative trends (dimming). Statistically significant trends are indicated by black dots.

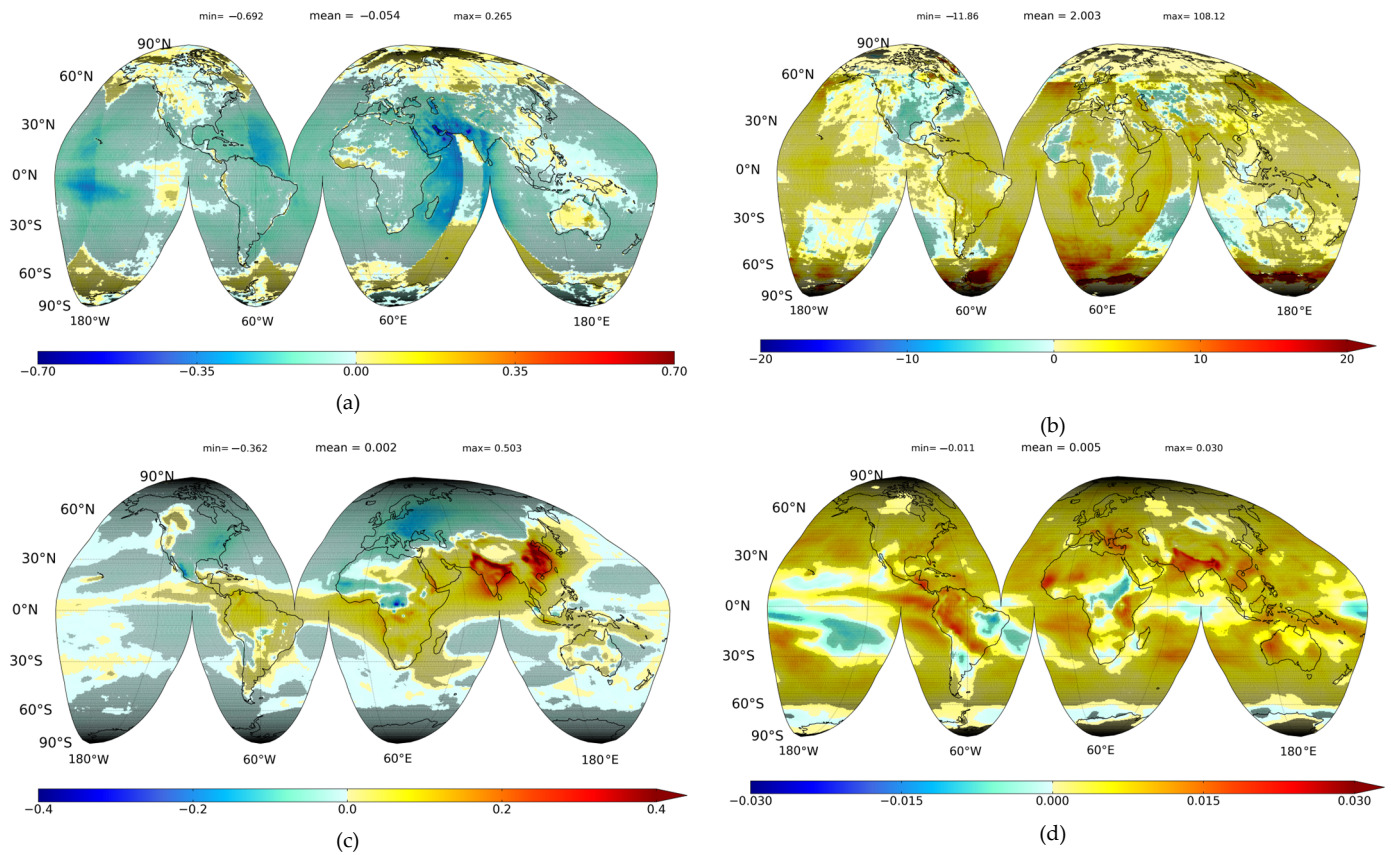


Figure S8. Global distribution of the changes of model input data that are relevant with SSR and GDB, namely of: total cloud cover (a), total cloud optical thickness (b), aerosol optical depth (c) and water vapor (d) over the period 1984-2018. Bluish colors indicate decreasing trends, while yellow-reddish colors correspond to increasing trends. The statistically significant trends are denoted with black dots.

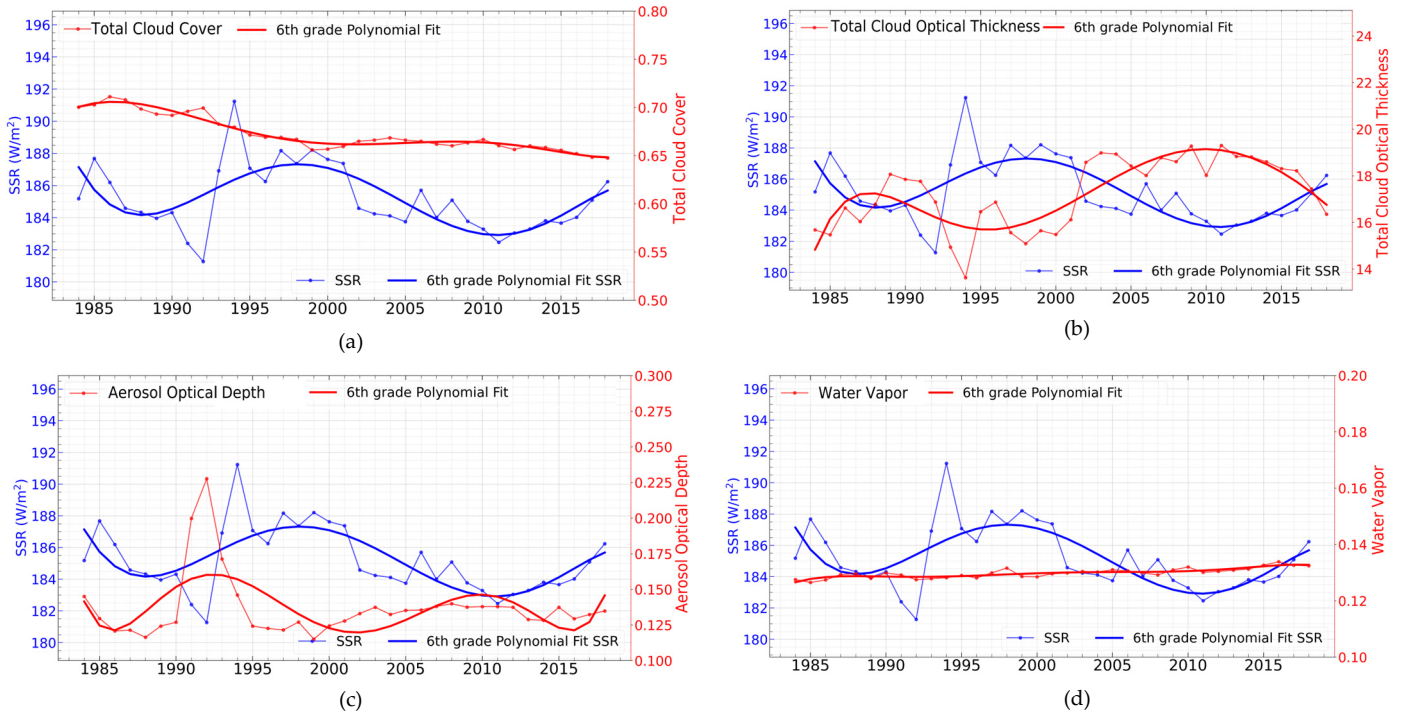


Figure S9. Time series of annual global mean SSR (in blue) and model input data (in red) which are relevant with GDB: total cloud cover (a), total cloud optical thickness (b), aerosol optical depth (c) and water vapor (d) over the period 1984–2018. The associated 6th grade polynomial fit lines are also shown.